

POLYMER BASED MORPHING SKIN FOR ADAPTIVE WINGS

Oliver Schorsch^{*}, Andreas Lühring[†], Christof Nagel^{††}, Rosario Pecora^{†††}, Ignazio Dimino^{††††}

^{*} Fraunhofer IFAM, Fraunhofer Institute for Manufacturing Technology and Advanced Materials
Wiener Straße 12, 28359 Bremen, Germany
oliver.schorsch@ifam.fraunhofer.de

[†] Fraunhofer IFAM, Fraunhofer Institute for Manufacturing Technology and Advanced Materials
Wiener Straße 12, 28359 Bremen, Germany
andreas.luehring@ifam.fraunhofer.de

^{††} Fraunhofer IFAM, Fraunhofer Institute for Manufacturing Technology and Advanced Materials
Wiener Straße 12, 28359 Bremen, Germany
christof.nagel@ifam.fraunhofer.de

^{†††} University of Naples - Federico II
Aerospace Engineering Dept. - Via Claudio 21, 80125 Naples, Italy
rosario.pecora@unina.it

^{††††} Italian Aerospace Research Center (CIRA)
Via Maiorise, 81043 Capua (CE), Italy
i.dimino@cira.it

Key words: Adaptive wing, trailing edge, morphing, elastomer, low temperature properties

Summary: *The development of elastomeric materials for adaptive wings focuses on the elasticity at -55 °C to ensure morphing at cruise altitudes. FEM simulations and mechanical tests are carried out to optimize fatigue and aging properties of this new multi-material device. Two large skin panels are manufactured and successfully assembled into a true-scale wind tunnel demonstrator for the experimental validation of adaptive trailing edge device functionality in simulated operative conditions.*

1 INTRODUCTION

Aerodynamic morphing for flight profile specific performance adjustment by changing surface area or camber has been used since the very beginning of aircraft industry. Nowadays, entirely mechanical actuation systems are established, where changes of surface area or angle/shape are obtained by moving solid elements. Well known examples are swing wing of fighter aircrafts, thrust vectoring of the Harrier or the movable engine of Osprey helicopters as well as slats, flaps and spoilers of every aircraft. [1]

Although widely used, moving solid elements has many disadvantages. Some solutions are quite complex like the trailing edge of the Boeing 747, too heavy or a gapless approach is

demanded for reduction of noise and fuel consumption. [2]

On the other hand seamless or gapless morphing is still a research topic. Gapless morphing combines an appropriate actuation system as well as a skin layer which is able to deform and to carry loads simultaneously. Many actuation systems have been discussed in the past, but there is no single material known yet that solves the mechanical paradox of morphing skins for aviation applications satisfactorily.

Most former morphing wing projects tried to implement large morphing areas, leading to heavy and expensive solutions. In the SARISTU project, funded from the European Union's Seventh Framework Programme, a new morphing approach was investigated focusing on the integration of smaller polymer based morphing elements to established structures like winglet and trailing edge. [3]

The SARISTU Adaptive wing Trailing Edge Device (ATED) was designed with reference to the outer wing of a CS-25 category aircraft. A polymer based morphing skin was developed by Fraunhofer IFAM to cover seamlessly a multi-finger ribs architecture enabling conformal and differential airfoil camber morphing. Wing shape is controlled during flight (cruise condition) in order to compensate the weight reduction following the fuel burning, by allowing the trimmed configuration to remain optimal in terms of efficiency (L/D ratio) or minimal drag (D). Trailing edge adaptations were investigated to achieve significant benefits in aircraft fuel consumption whose reduction may range from 3% to 5% due to the improved aerodynamic efficiency.

2 RIB BASED MORPHING TRAILING EDGE

In order to enable the transition of the adaptive trailing edge sections from the reference (baseline) shape to the target ones, a morphing structural concept was developed (by UNINA) for the ATED ribs. Each rib (Figure 1) was assumed to be segmented into four consecutive blocks (B0,B1,B2,B3) connected to each other by means of hinges located on the airfoil camber line (A,B,C). Block B0 is rigidly connected to the rest of the wing structure, while all the other blocks are free to rotate around the hinges on the camber line, thus physically turning the camber line into an articulated chain of consecutive segments. Linking rod elements (L1,L2) -hinged to not adjacent blocks- force the camber line segments to rotate according to specific gear ratios.

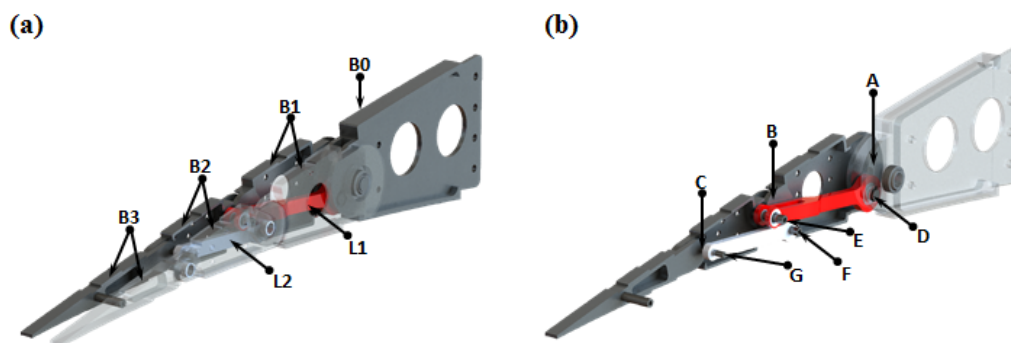


Figure 1: Morphing rib architecture: (a) blocks and links, (b) hinges.

These elements make each rib equivalent to a single-DOF mechanism: if the rotation of any of the blocks is prevented, no change in shape can be obtained; on the other hand, if an actuator moves any of the blocks, all the other blocks follow the movement accordingly. The rib mechanism uses a three segment polygonal line to approximate the camber of the ATED airfoil and to morph it into the desired configuration while keeping approximately unchanged the airfoil thickness distribution. An inverse kinematic problem was addressed to properly define the positions of all the hinges of the mechanism; the positions of the hinges along the camber line (both in un-morphed and morphed configurations) represented the input data of the problem, they were fixed by imposing equal chordwise extensions for the blocks B1,B2,B3; the positions of the links (i.e. of the hinges D,E,F,G) were considered as the unknown variables to be determined. The ribs' kinematic was transferred to the overall trailing edge structure by means of a multi-box arrangement (Figure 2). Each box of the structural arrangement was assumed to be characterized by a single-cell configuration delimited along the span by homologue blocks belonging to consecutive ribs, and along the chord by longitudinal stiffening elements (spars and/or stringers).

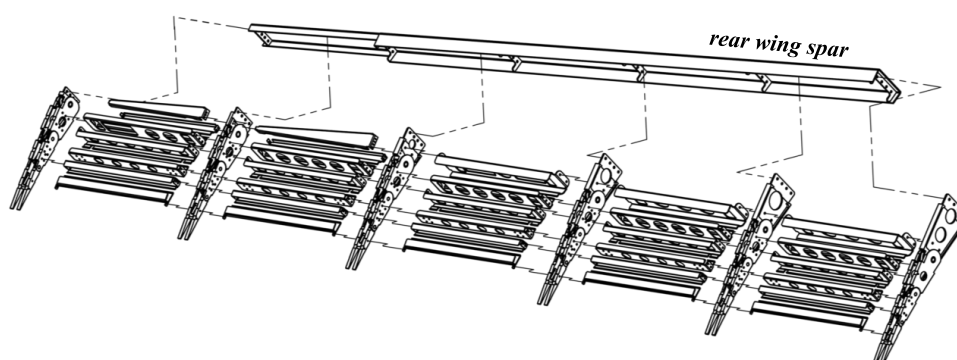


Figure 2 : Morphing box architecture (exploded view).

Upon the actuation of the ribs, all the boxes are put in movement thus changing the external shape of the trailing edge (Figure 3); if the shape change of each rib is prevented by locking the actuation chain, the multi-box structure is elastically stable under the action of external aerodynamic loads.

Fast and reliable numerical methods combined with rational design criteria were implemented to assess the preliminary sizing of the ATE primary structure with reference to the most severe load condition expected in service (limit load condition); AL2024-T5 alloy was used for spars, stringers and rib plates, while 17-4PH steel was used for ribs' links. Off-the-shelf airworthy components were properly selected for hinges and bushings. The resulting structural layout was analyzed by means of advanced finite element analyses which proved:

- the capability of the structure to enable morphing through smooth rigid-body kinematic of the embedded mechanisms;
- the absence of any local plasticization and elastic instability at limit load condition;
- the absence of any failure up to the ultimate load condition (i.e. limit loads multiplied by an amplification factor equal to 1.5).



Figure 3 : ATE configurations: morphed up (left hand side), morphed down (right hand side).

3 MORPHING SKIN DESIGN

The primary challenge for adaptive wings is to find a skin design that is able to deform and to carry aerodynamic loads simultaneously. One solution to solve this mechanical paradox is the development of a multi-material skin consisting of hard and soft segments. While soft skin segments release a smooth, gapless transition between movable and fixed parts of the underlying kinematic structure hard skin segments compensate deformations due to air pressure gradients (Figure 4).

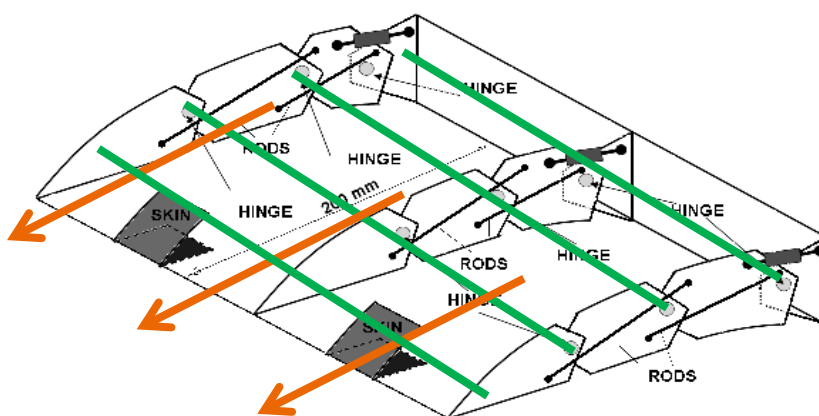


Figure 4: One solution to solve the mechanical paradox of morphing skins is to transmit loads in spanwise direction and to allow morphing via chordwise movement.

The design of such skin is shown in Figure 5. The soft segments are based on elastomer foam while the hard segments consist of aluminium profiles. Both segments are covered by a thin layer to ensure a smooth surface. The soft segments are located above and under the rib hinges while the hard segments are connected to the rib structure.

The morphing skin is able to follow the movement which is prescribed by the active ribs while maintaining the conformity in the deflected configuration for aerodynamic reasons.

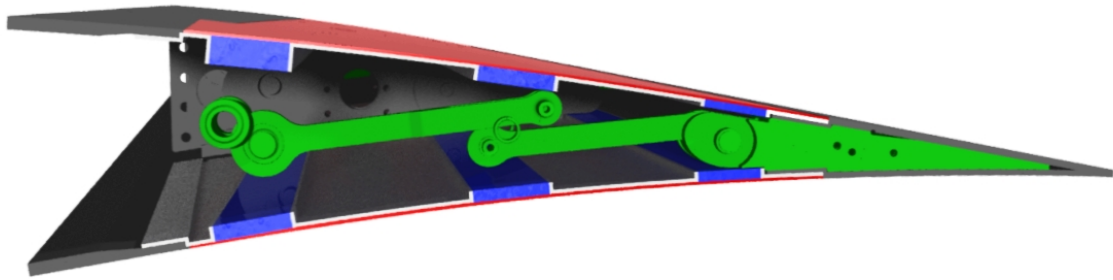


Figure 5: The morphing skin consists of hard and soft segments. Elastomer foam (blue) is used for soft segments which are located above and under the rib hinges. Hard segments are aluminium profiles (grey). Hard and soft segments are covered with a thin elastomer layer (red). The rib kinematic is shown simplified (green).

The elastomer foam geometry was FEM optimized in respect to the required strain and compression for morphing and to minimize shape deviations due to aerodynamic loads.

Longer foam regions in chordwise direction lead to lower stress and improve fatigue life of the elastomer foam, but buckling caused by aerodynamic suction increases. The foam thickness was calculated to reduce buckling to less than 1 mm height during cruise flight conditions.

Upper and lower skin side is attached to stringers located between the active ribs (s. Figure 6) to transmit load in spanwise direction and to assure attachment/ detachment for ease of maintenance and repair.

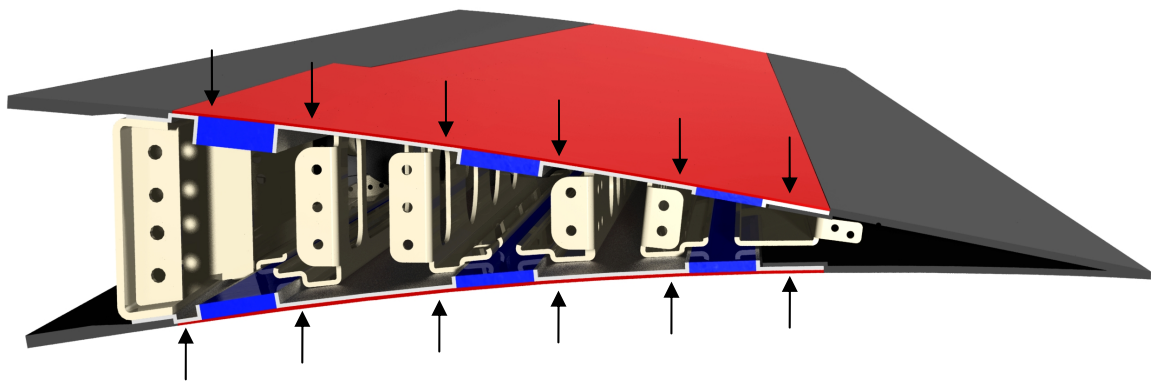


Figure 6: Upper and lower skin side are connected to stringers located between the ribs.

4 LOW TEMPERATURE ELASTOMERS

In order to maximize the durability of an elastomer based morphing skin different material properties are required. Most importantly a material is needed, that show almost constant compression and tension properties as well as storage modulus over the whole temperature range of an aircraft wing surface (-55 °C to 80 °C) and over a very large number of temperature cycles.

Furthermore environmental resistances (weather, UV radiation), chemical resistance (Skydrol, deicing agent) as well as resistance to abrasion (sand, small stones on runway) are essential.

The strain within the soft skin segments, given by geometry and deflection angle of the morphing trailing edge, is of great importance for the material selection as well. Maximum strain must not exceed 10 % otherwise the elastomer would fail due to fatigue after a number of loading cycles. More than 100000 cycles is expected to be sufficient for a full service time of a common aircraft.

Finally, high adhesion strength between elastomer skin layer, elastomer foam and aluminium parts is essential for load transmission between hard and soft segments.

Many elastomers are certified for aircraft applications. Examples are silicone, EPDM and polysulfide, which are used as sealants, but not for high strain. One reason is the loss of elasticity as soon as environmental temperature falls below the glass transition temperature of the elastomer (usually between -45 °C and -10 °C, Figure 7).

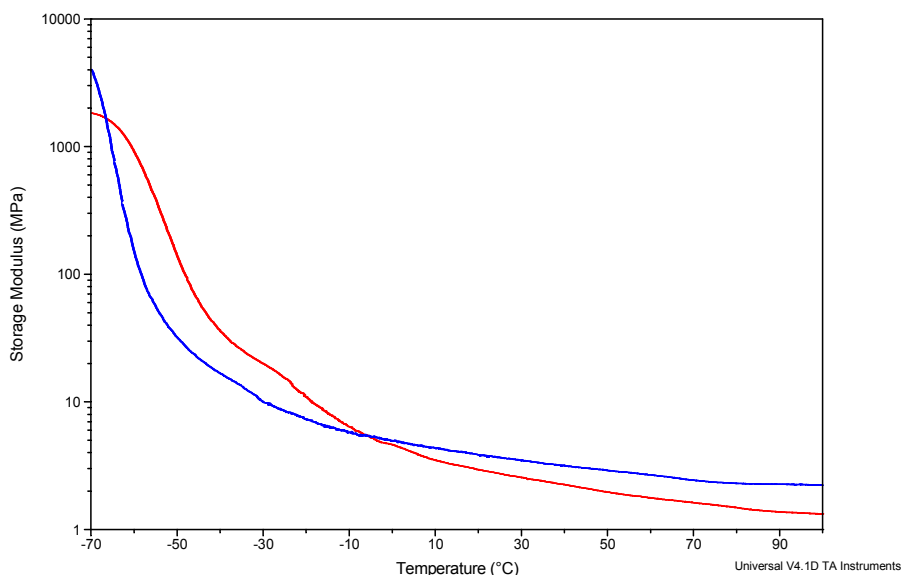


Figure 7: Dynamic mechanical analysis of low temperature polyurethane Sikaflex 553 (Sika, blue) and EPDM sheeting (Dr. D. Müller, red).

Silicone elastomers are an exception providing excellent elasticity over a wide temperature range. Among the variety of silicone elastomers polydimethylsiloxane (PDMS) is the most used silicone for technical applications. Fluorosilicone is based on

polytrifluoropropyl-methylsiloxane and is used for applications that require fuel or hydrocarbon resistance.

Although glass transition temperature of these silicones is well below $-100\text{ }^{\circ}\text{C}$, common PDMS and fluorinated silicone lose flexibility below $-35\text{ }^{\circ}\text{C}$ due to cold crystallization of polymer segments. Crystallization can be reduced or even inhibited by substitution of functional groups at polymer side chains. Polydimethyldiphenylsiloxane (PDMDPS) is the most important crystallization hindered silicone. Because of almost constant elasticity between $100\text{ }^{\circ}\text{C}$ and $-100\text{ }^{\circ}\text{C}$ phenylated silicone is an important encapsulation material for space applications (Figure 8).

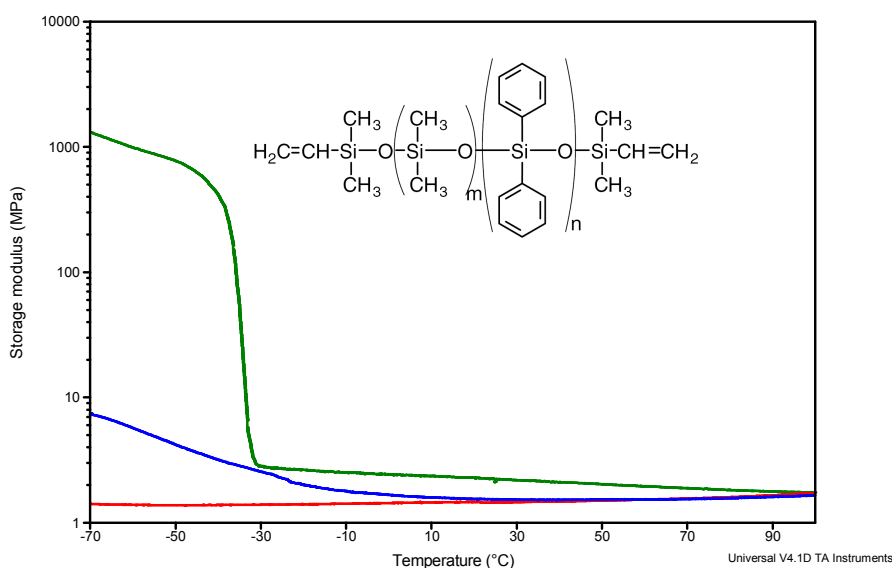


Figure 8: Dynamic mechanical analysis of common silicone sheeting (MVQ Silicones GmbH, green, $n=0$) and low temperature silicones with different methyl/phenyl ratio (m/n), Sylgard 184 (Dow Corning blue), Elastosil S690 (Wacker, red).

Several commercial low temperature silicones are available, mostly for space industry or other low temperature applications. Most of low temperature silicones are either platinum catalyzed or peroxidized cured products. Unfortunately no commercially available low temperature silicone sheets and foams meet all the needed material properties for a morphing skin and are known to be very difficult to bond by adhesives.

Hence, in order to adjust the needed material properties and to maximize the adhesion strength between all material interfaces of the morphing skin it was decided to tailor reactive formulations of platinum catalyzed low temperature silicones. These tailored reactive formulations can be cured or foamed to obtain the required low temperature silicone component.

One important example is the addition of fumed silica which improves tensile strength, elongation properties, tear strength and adjusts the viscosity of the formulation at the same time.

The effect of fumed silica on tear strength is shown in Figure 9. Different levels of Evonik AEROSIL R 8200 were added to the low temperature silicone encapsulants Momentive 655 and Dow Corning 3-6121. In opposite to the Momentive encapsulant Dow Corning 3-6121 contains already an unknown amount of fumed silica. All formulations were cured 1 h at 100 °C and the testing was carried out according DIN 53515 using Graves angle test piece.

Fumed silica concentration more than 15 % improves several mechanical properties of the cured silicone elastomers (“locking effect”) but the increased formulation viscosity makes processing more difficult or even impossible.

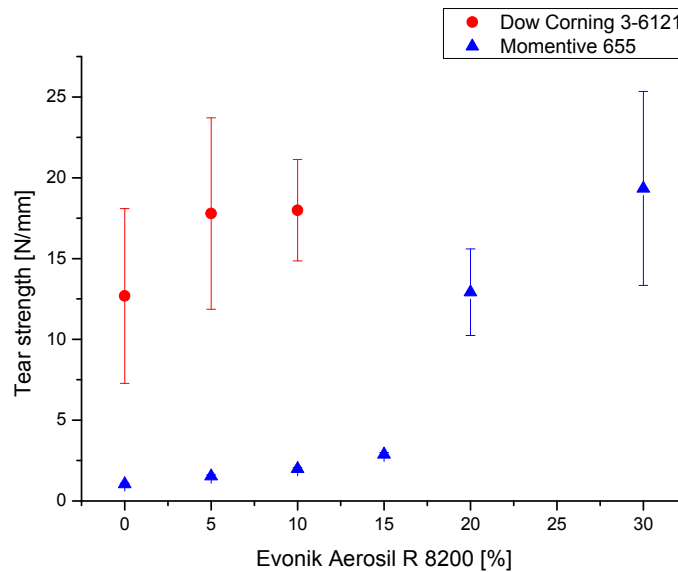


Figure 9: Effect of fumed silica on tear strength of different low temperature silicones.

Liquid formulations of reactive silicone are difficult to foam without special foaming equipment. One possibility is the addition of physical or chemical foaming agents. While chemical foaming agents are thermal reactive components physical foaming agents consists of encapsulated low-boiling solvents. Both foaming agents release gas after reaching a critical temperature. Since curing reaction and foaming reaction occur at the same time, the formulation must be tailored specifically. The speed of crosslinking reaction can be adjusted by adding inhibitors or crosslinking catalyst.

5 MECHANICAL PROPERTIES

Since elasticity and strength properties have to be constant at high and low temperature, the tailored low temperature silicones were tested under quasi-static and fatigue loading at -55 °C, 23 °C, and 80 °C.

Quasi-static tests were performed in uniaxial tension and uniaxial compression at a strain rate of ~0.1/s. The shape of the tensile test samples was similar to geometry 5A in ISO 527-2. In compression, cylinders with 10 mm height and 20 mm diameter were used. Results are shown in Figure 10. Considering the slope of the stress-strain curves, it can be confirmed that

the stiffness is almost constant over the whole temperature range. A decrease in static tensile strength with increasing temperature can be noticed, but this is not of concern because structures are designed for fatigue loads, which are far below the static limit. Based on the stress-strain curves in Figure 10, a hyperelastic material model was calibrated, which was later on used to describe the material properties within finite element simulations.

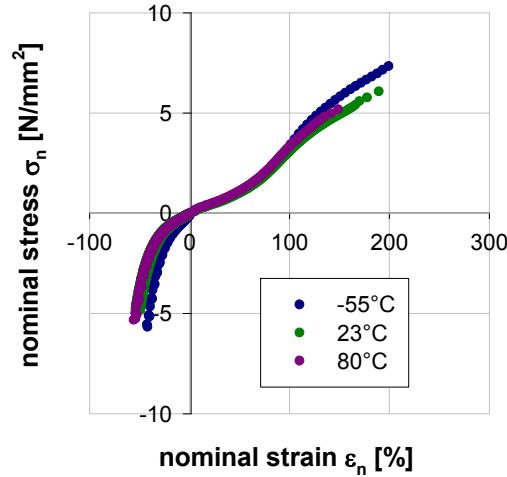


Figure 10: Stress-strain curves from uniaxial tension and uniaxial compression tests at indicated temperatures and a strain rate of 0.1/s.

T-joints as depicted in Figure 11 were used for fatigue tests at test frequencies between 3/s and 7/s and a load ratio of $R=-1$. The objective of these tests was to set up a strain-life (E-N) curve in order to estimate the fatigue life of the skin module based on finite element modeling with statistical significance. The face-to-face distance of the foam segments between the aluminium parts was ~ 30 mm and the thickness was ~ 10 mm. The sample width was ~ 35 mm and the thickness of the elastomeric top layer was ~ 1 mm. Nominal strain was defined as change in length divided by the initial face-to-face distance of the foam segments. Results are presented in Figure 11 as nominal strain amplitude vs. number of cycles to failure. At lower strain amplitudes, the number of cycles to failure refers to visible crack initiation. No significant crack propagation phase was visible at higher strain amplitudes, so the number of cycles refers to total failure. Visual fracture surface inspection indicated predominantly cohesive failure within the foam segments.

The dashed line in Figure 11 refers to a power law

$$(1) \quad \varepsilon_a = \varepsilon_{a0} \cdot N_f^{-1/k}$$

as fitted to experimental data, where ε_a denotes nominal strain amplitude, N_f denotes number of cycles to failure, and ε_{a0} and k are material-dependent parameters. Since ε_a acts as controlled variable and N_f as dependent variable, Eq. (1) was resolved for N_f and subsequently least-squares fitted to measured N_f as function of applied ε_{a0} , assuming a lognormal distribution of measured N_f . The values of the corresponding fit parameters are $\log \varepsilon_{a0} = (2.34 \pm 0.12)$ (units of ε in %) and $k = (4.63 \pm 0.47)$.

A lower tolerance limit was calculated based on a t-distribution for $\log N_f$, with a survival probability of $P=95\%$ and $n-2$ degrees of freedom. This procedure is similar to the one outlined in ISO 12107. Based on the lower tolerance limit, which is shown as a full line in Figure 11, it can be stated that the joint can withstand approximately 250 000 cycles at a nominal strain amplitude of 10 % until crack initiation. At a nominal strain amplitude of 5 %, the joint can withstand approximately 5 000 000 cycles. If a specified number of cycles of $N = 20\,000$ is considered, which corresponds to the expected number of the ATED operation cycles, the strain amplitude could be as high as approximately 17 %, which is three times as high as the expected strain maximum occurring in operation. It can hence be concluded that, under the current state of knowledge, the skin of the ATED is fail safe.

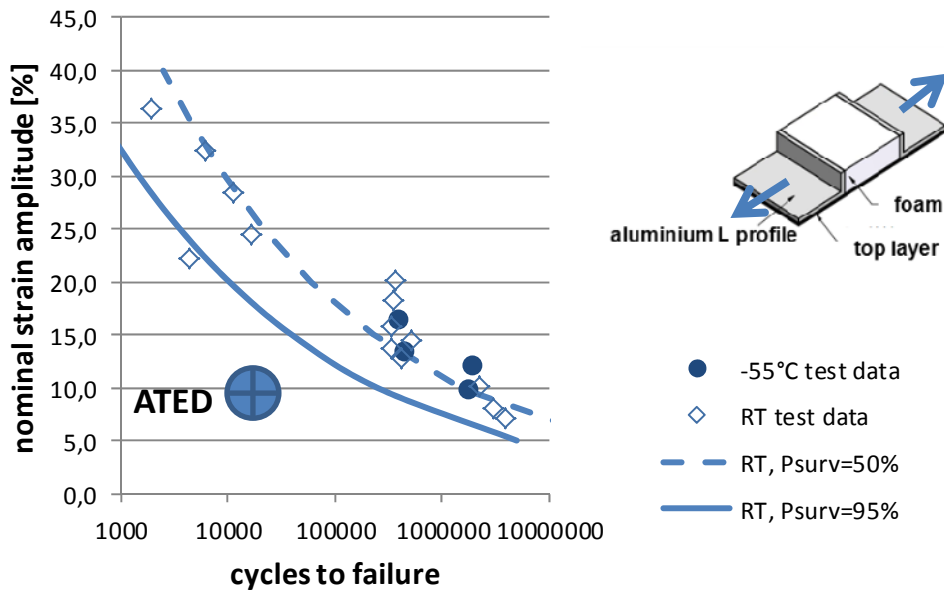


Figure 11: Strain-Life ($E-N$) curve generated from T-joint fatigue test data at room temperature (RT).

6 SKIN MANUFACTURING

The morphing skin consists of the three main components. The space between the aluminium profiles is filled with low temperature foam. Aluminium profiles and foam are covered with a protective layer of low temperature silicone elastomer (s. Figure 12).

Due to the unavailability of appropriate adhesives to bond those materials for low temperature purposes a new manufacturing process was developed. Core feature of this process is to perform the foaming, curing and adhesive bonding of different reactive silicone formulations and aluminium profiles at the same time.

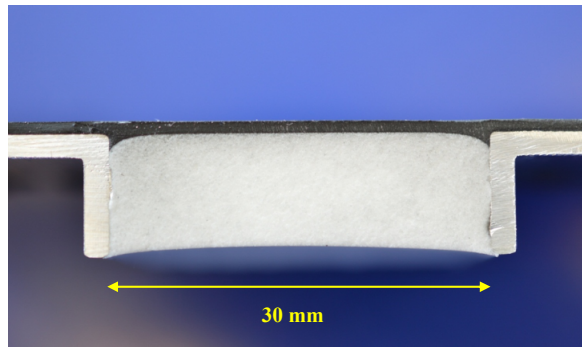


Figure 12: The morphing skin consists of aluminium profiles, low temperature silicone foam and a protective layer of low temperature silicone elastomer.

Figure 13 shows a sketch of a heating device to manufacture morphing skins up to 2.3 m length. The heating device consists of several heating pads which are separately controlled to obtain a homogenous temperature distribution and can reach temperatures up to 150 °C.

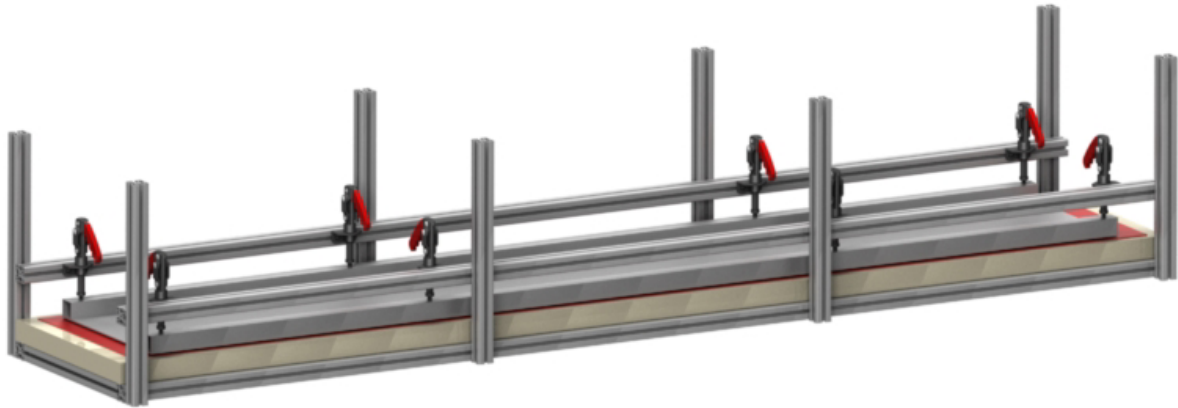


Figure 13: 2.8 m large heating device to process curing, foaming and adhesive bonding of morphing skin components at the same time.

During the SARISTU project several large skin panels were manufactured and successfully assembled into a true-scale wind tunnel demonstrator (s. Figure 14).

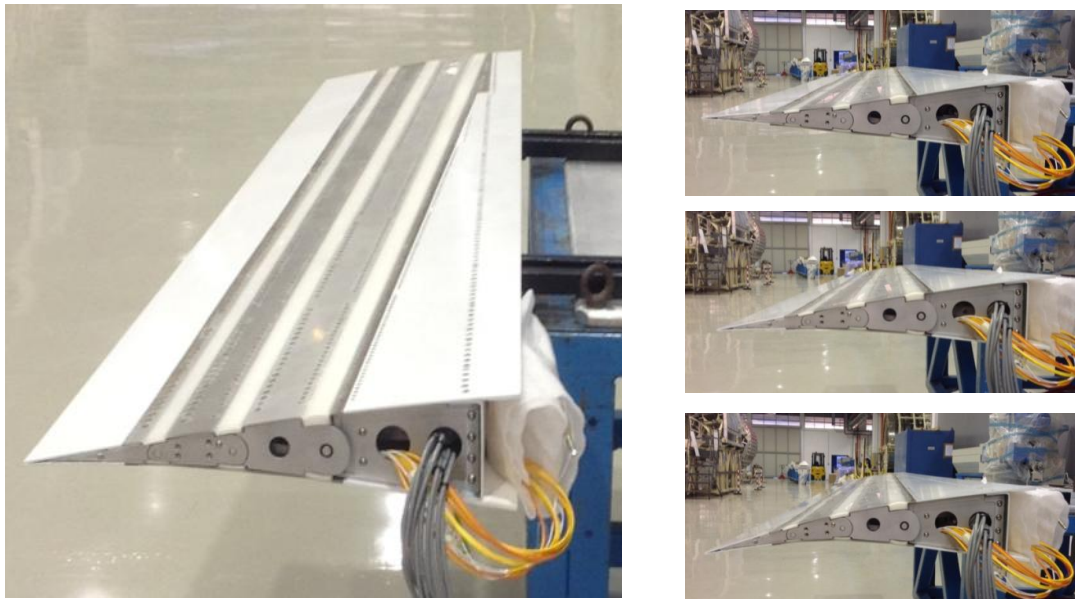


Figure 14: SARISTU adaptive trailing edge containing morphing skins at upper and lower side.

The experimental validation of adaptive trailing edge device functionality in simulated operative conditions is planned at TsAGI (Moscow) after the integration to the SARISTU morphing wing which consists of an adaptive leading edge, a morphing trailing edge and adaptive wingtip (s. Figure 15).



Figure 15: SARISTU morphing wing consists of different morphing devices which functionality will be tested in a windtunnel test at TsAGI, Moscow.

7 CONCLUSIONS

An elastomer based skin for seamless morphing of a rib based adaptive trailing edge was developed. The skin material development focused on low temperature requirements for cruise flight conditions, resistance to environmental conditions as well as long fatigue life.

Several large skin panels were manufactured in a newly developed moulding process where all skin components are cured, foamed and bonded at the same time to maximize the adhesive bonding between all material interfaces.

Several skins are successfully assembled into a true-scale wind tunnel demonstrator for future functionality tests in simulated operative conditions.

The research leading to these results has gratefully received funding from the European Union's Seventh Framework Programme for research, technological development and demonstration under grant agreement no 284562.

REFERENCES

- [1] C. Thill, J. Etches, I. Bond, K. Potter, P. Weaver, Morphing Skins, *The Aeronautical Journal*, March 2008, Paper no. 3216
- [2] P.K.C. RUDOLPH, High-lift systems on commercial subsonic airliners, *NASA Ames Research Center*, 1996, Moffet Field, CA, USA.
- [3] <http://www.saristu.eu/>